Real-World Quantum Sensors: Evaluating Resources for Precision Measurement

Nicholas Thomas-Peter,[1] Brian J. Smith,[1] Animesh Datta,[1] Lijian Zhang,[1] Uwe Dorner,[2,1] and Ian A. Walmsley[1]

[1]*Clarendon Laboratory, Department of Physics, University of Oxford, OX1 3PU, United Kingdom*

[2]*Centre for Quantum Technologies, National University of Singapore, 3 Science Drive 2, 117543 Singapore, Singapore*

(Received 17 May 2011; published 8 September 2011)

Quantum phenomena present in many experiments signify nonclassical behavior, but do not always imply superior performance. Quantifying the enhancement achieved from quantum behavior needs careful analysis of the resources involved. We analyze the case of parameter estimation using an optical interferometer, where increased precision can in principle be achieved using quantum probe states. Common performance measures are examined and some are shown to overestimate the improvement. For the simplest experimental case we compare the different measures and exhibit this overestimation explicitly. We give the preferred analysis of these experiments and calculate benchmark values for experimental parameters necessary to realize a precision enhancement. Our analysis shows that unambiguous real-world enhancements in optical quantum metrology with fixed photon number are yet to be attained.

DOI: 10.1103/PhysRevLett.107.113603 PACS numbers: 42.50.Dv, 03.67.Bg, 06.20.−f, 42.50.Ex

Quantum-enhanced technologies such as quantum computing, cryptography and metrology utilize nonclassical behavior of quantum systems to surpass the performance of their classical analogs. Often signatures of quantum behavior such as violation of a Bell inequality, photon antibunching, or sub-Poissonian number statistics are observed in an experiment. In some cases, their presence may be sufficient to ensure superior performance of the quantum protocol over the classical. There are situations, however, in which quantum behavior does not necessarily imply performance beyond classical limits and further analysis is necessary to ensure improvement.

Quantum sensing employs quantum probes to estimate a parameter with precision beyond what is possible with classical resources [1]. Analyzing the limits on precision is of both practical and fundamental interest, requiring careful accounting of the necessary resources to compare classical and quantum protocols. Entangled states of multiple particles are a critical component in enabling quantum enhancement in many situations [2], as are detectors that extract maximum information about the parameter of interest [3]. Calculating the precision that can be achieved for fixed resources provides a basis for comparing quantum and classical protocols. Recent work has shown that practical imperfections such as loss, decoherence, state-preparation, and detector inefficiency decrease the enhancement of quantum metrology protocols [4–6]. Thus poor enumeration, which distorts the resources used and hence the enhancement obtained, is problematic.

Several proof-of-principle experiments aimed at quantum-enhanced parameter estimation have been performed to date [7]. Many utilize nonclassical signatures in detection outcomes to indicate improved precision. However, as we will show, this is insufficient to demonstrate increased precision beyond the classical limit and further information is necessary to accurately compare quantum and classical strategies.

In this Letter, we address the gap between proofs-of-principle and issues of practice by examining a quantum sensor based on optical interferometry. We develop a bound on the achievable precision based on the well known classical and quantum Fisher information. In contrast to previous analyses however, we incorporate imperfections at all stages of the experiment. When these imperfections are present, we show that quantum enhancement can be overestimated by improper resource accounting. To experimentally demonstrate this we construct a source of heralded entangled states, generating with it the simplest quantum states which ideally lead to improved precision, and examine the behavior of different enhancement measures including supersensitivity [8]. The heralded state is fully characterized, including all photon number subspaces, using a novel tomographic technique. This allows us to account for all the consumed resources. We show that this state, although beating previously applied classical limits, cannot beat our bound.

To estimate the phase ϕ in a two-mode interferometer, a state $\hat{\rho}$ is launched into it, evolves into the state $\hat{\rho}(\phi)$ due to interaction with the phase-shifting element, and a measurement is performed at the sensor output. The phase ϕ is estimated from the outcomes of ν repeated experimental trials. We define the average number of photons at the interferometer *input*, $N = \langle \hat{n} \rangle$, and the total number of experimental trials, ν, necessary to achieve a given level of phase precision, $\Delta\phi$, as the resources. For fixed resources, we then compare the precision of the quantum and classical approaches and the approach with the smallest phase uncertainty is thus the better strategy.

Two effects attributed to quantum behavior in interferometry are phase super-resolution and phase supersensitivity. Phase super-resolution, the sinusoidal variation of an

N-fold detection signal as a function of interferometer phase ϕ with an N-times increase in oscillation rate, can be observed using only classical input states of light and projective measurements [8]. Recently, the visibility of such super-resolving fringes was shown to be able to distinguish between quantum and classical input states of a Mach-Zehnder interferometer [9]. This signature of quantum behavior does not, however, quantify improved performance beyond classical interferometry.

Phase supersensitivity, a commonly employed measure of performance, is defined as reduced phase uncertainty compared to that possible with classical resources [8]. The model in [8] incorporates experimental imperfection through "efficiency" and visibility parameters η_p and V, by means of a phenomenological model of an N_d-fold detected coincidence signal. Here, η_p is the proportion of the input state $\hat{\rho}$ that can lead to an N_d-fold detection event. The visibility is required to satisfy $\eta_p V^2 N_d > 1$ in order for the measurement to be regarded as "supersensitive." However, this assumes unit sensor transmission and perfectly efficient detectors. It includes only imperfect state preparation; with $N_d = N$, the number of input photons. In fact, the most common experimental situation is that $N_d < N$ so that the resources consumed are significantly underestimated. Claims of precision beyond the classical limit that utilize this measure must therefore be interpreted carefully.

In general, the precision of the phase estimate is limited by the Cramér-Rao bound (CRB) [3], $\Delta\phi \geq 1/\sqrt{\nu F(\phi)}$, where $F(\phi) = \sum_j (1/p_j(\phi))|\partial p_j(\phi)/\partial\phi|^2$, is the Fisher information (FI). The probability $p_j(\phi)$ corresponds to an outcome j of a measurement. $F(\phi)$ is bounded from above by the quantum Fisher information (QFI), F_Q, found by maximizing $F(\phi)$ over all physical measurements. Hence the quantum Cramér-Rao bound (QCRB), $\Delta\phi \geq 1/\sqrt{\nu F_Q(\phi)}$, depends only on the input state and channel, independent of measurement [3].

Ideally, the QCRB of N uncorrelated photons leads to the standard quantum limit $\Delta\phi \geq \Delta\phi_{\mathrm{SQL}} = 1/\sqrt{\nu N}$, equivalent to the precision attained with a coherent state of unknown phase with average photon number $|\alpha|^2 = N$. When quantum input states are employed, the best attainable precision is given by the so-called Heisenberg limit $\Delta\phi \geq \Delta\phi_{\mathrm{HL}} = 1/\sqrt{\nu}N$ which is achieved by the $N00N$ state [7–10]. Note that to reach this precision, an appropriate optimal detection scheme with unit efficiency must be used. However, if the sensor has finite transmissivity η, assumed equal in both interferometer arms, the classical strategy is bounded by the standard interferometric limit (SIL) $\Delta\phi \geq \Delta\phi_{\mathrm{SIL}} = 1/\sqrt{\nu\eta N}$ [4]. $N00N$ states are extremely susceptible to loss; removal of even one photon results in a phase-insensitive state. The QFI for $N00N$ states through the same channel is thus scaled by the probability that all photons are transmitted, η^N, giving a QCRB of $\Delta\phi \geq 1/\sqrt{\nu\eta^N N}$.

For $N00N$ states, an optimal measurement is projection onto $|\Psi_\pm\rangle = (|N,0\rangle \pm |0,N\rangle)/\sqrt{2}$, where $|m,n\rangle$ denotes m (n) photons in each mode of the interferometer. This measurement set has three possible outcomes: $j = \pm$ (detection of $|\Psi_\pm\rangle$) and $j = 0$ (otherwise). In practice, it is difficult to realize single-mode sensors and this may lead to nonideal interference due to unmeasured distinguishing information. Measurement outcomes therefore typically have probabilities $p_\pm(\phi) = f[1 \pm V\cos(N\phi)]/2$ and $p_0(\phi) = 1 - p_+(\phi) - p_-(\phi)$, leading to a CRB $\Delta\phi \geq \Delta\phi_{\mathrm{min}} = 1/\sqrt{\nu f}NV$ [11]. Here, $f = \eta_p(\eta\eta_d)^N$, where η_d is detector efficiency, and V is the interference visibility accounting for multimode states and detectors. The state is said to exhibit super-resolution if $p_\pm(\phi)$ oscillates N times the applied phase. To surpass the SIL requires $\Delta\phi_{\mathrm{min}} < \Delta\phi_{\mathrm{SIL}}$, leading to a threshold visibility

$$V_{\mathrm{th}} = \sqrt{\eta/fN}, \tag{1}$$

which is equivalent to that in [8] with $\eta = \eta_d = 1$ and $N = N_d$. A state is said to exhibit supersensitivity if $V \geq V_{\mathrm{th}}$, and the classical precision limit is surpassed.

The FI and QFI analyses give a straightforward method to quantify the resources consumed in an experiment and compare quantum with classical strategies. The QFI reveals whether or not the classical limit could be beaten in principle using a particular state and channel, while the FI reveals whether or not it can be beaten with the addition of a particular measurement. To ascertain the best performance of a given quantum strategy, one must therefore know the density matrix $\hat{\rho}$ of the input state, when it is prepared, as well as the device transmission and detector efficiency, giving N, ν, the QFI, and the FI, respectively. In our case, $\hat{\rho}$ will be obtained through state tomography and ν by heralded state preparation.

A common practice is to "post-select" on particular measurement outcomes and neglect the occurrence of others, including when nothing is detected at the output. This amounts to setting η_p, η, η_d to 1 and $N = N_d$. This neglects both ν and the true N, significantly underestimating the exponentially growing number of trials [11] and information from neglected measurement outcomes.

To experimentally examine realistic quantum sensors, we implement the simplest case, employing two-particle states, in which increased precision can be shown. We use an optical sensor design based on a heralded two-photon Holland-Burnett (HB) state [11,12]. HB($N = 2k$) states are prepared by launching k photons in both input ports of a 50:50 beam splitter. The HB(2) state provides the laxest constraints on sensor transmissivity and detection efficiency [4,5]. Furthermore, the optimal measurement for phase estimation using HB states can be implemented with realistic number-resolving detection [5]. The QCRB of a HB state in the lossless case is $\Delta\phi \geq 1/\sqrt{\nu N(N/2+1)}$ which, for large N, has Heisenberg scaling that differs only

by a constant factor. With loss this state retains phase sensitivity and precision enhancement far better than $N00N$ states [13]. Indeed, the QCRB for the HB state approximately follows the optimum value for a wide range of η, η_d and N [4,5].

The scheme used to generate heralded HB states is shown in Fig. 1(a). A polarization-based N-photon HB state is obtained by combining two orthogonally polarized $k = N/2$-photon Fock states at a polarizing beam splitter [11]. The required Fock states are generated by two parametric down-converters (PDC), where k photons in one mode of each PDC are heralded by detecting k photons in the other mode. The PDCs are designed to produce spectrally disentangled modes [14] to avoid the compromise of state purity due to heralding, which is crucial for high-visibility interferometry. As spectral filtering is not required to increase the state purity, the preparation efficiency is determined solely by the system loss. In principle this source, with the use of photon-number-resolving heralding detectors [15], generates ideal HB states of arbitrary N.

The quality of the heralded Fock states used to generate the HB(2) state, $(|2,0\rangle - |0,2\rangle)/\sqrt{2}$, was tested by means

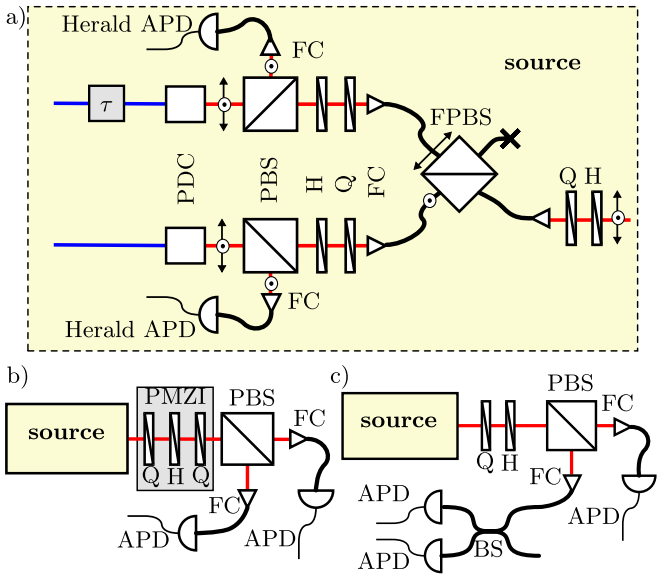

FIG. 1 (color online). Setup for generating and characterizing heralded HB states. (a) State generation based on two parametric down-converters (PDC). Half- (H) and a quarter-wave plates (Q) after each polarizing beam splitter (PBS) adjust the polarizations to combine photons at a fiber polarizing beam splitter (FPBS). Coincidence detection between heralding avalanche photodiodes (Herald APDs) signals HB state preparation at the output of the FPBS. (b) PMZI applies phase ϕ between $\pm 45°$ polarizations. Coincidence detection between the APDs implement optimal measurement for HB(2) state. (c) Tomography uses a quarter- (Q) and half-wave plate (H) followed by a PBS. Outputs are coupled into single-mode fiber (FC) with the reflected mode split by a 50:50 fiber beam splitter (FBS) for partial number resolution.

of Hong-Ou-Mandel interference between heralded single photons [Fig. 2(a)]. The theoretical fit gives a visibility of $90 \pm 3\%$ ($80 \pm 3\%$ raw), setting a lower bound on the input photon purity and distinguishability, and an upper bound for the multiphoton fringe visibility in Eq. (1). The residual impurity is partly intrinsic [14] and partly due to imperfect compensation of the optical fiber birefringence.

We reconstruct the full heralded state thorough state tomography using the experimental arrangement shown in Fig. 1(c) [11,16]. Population in lower photon number subspaces arises from loss so that coherences between subspaces of different photon number can be neglected. Figure 3(a) shows the reconstructed density matrix. The heralded state has populations of 0.686, 0.277, and 0.037 in the zero-, one-, and two-photon subspaces giving an average photon number of 0.35. This state has an overlap of 0.031 with the ideal two-photon HB state, while the renormalized two-photon subspace has an overlap of 0.85.

The heralded HB states are launched into a polarization Mach-Zehnder interferometer, PMZI in Fig. 1(b), which introduces a controllable relative phase between the two modes. Figure 2(b) shows the detection count-rate phase dependence for heralded single-photon states (dashed) and heralded HB(2) states (solid). Theoretical fits show visibilities of $90.9 \pm 0.5\%$ and $80.6 \pm 1.5\%$ ($76.4 \pm 1.4\%$ raw), respectively. The latter is consistent with the measured state purity.

For $N = 2$, HB and $N00N$ states are equivalent and Eq. (1) can be applied. Using post-selection, only data resulting in twofold outcomes are recorded, η and f are set to 1, and $N = 2$, yielding a threshold visibility $V_{\text{th}} = 1/\sqrt{2}$. The measured fringe visibility significantly exceeds this bound and so by this analysis we achieve supersensitivity, beating the SQL. If we renormalize the post-selected photon number subspace and use $\eta_p = 0.85$ while still neglecting η and η_d, we obtain $V_{\text{th}} = 0.77$. Our measured fringe visibility also exceeds this threshold, again demonstrating supersensitivity and beating the SQL. Since the

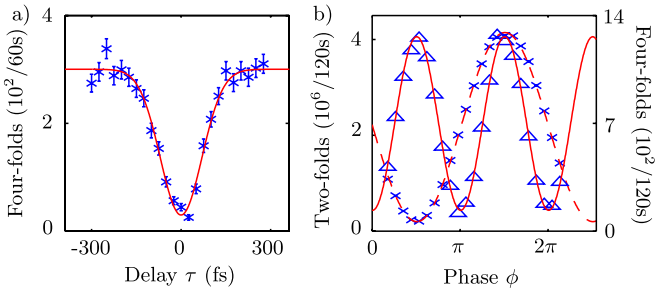

FIG. 2 (color online). Quantum interference of heralded photonic states. (a) Hong-Ou-Mandel interference between two heralded single photons as a function of delay, τ. (b) Setting $\tau = 0$ and scanning the PMZI phase shows two-photon (solid) and single-photon (dashed) interference. Error bars are derived from Poissonian statistics and contributions from multiple PDC pair emissions are removed.

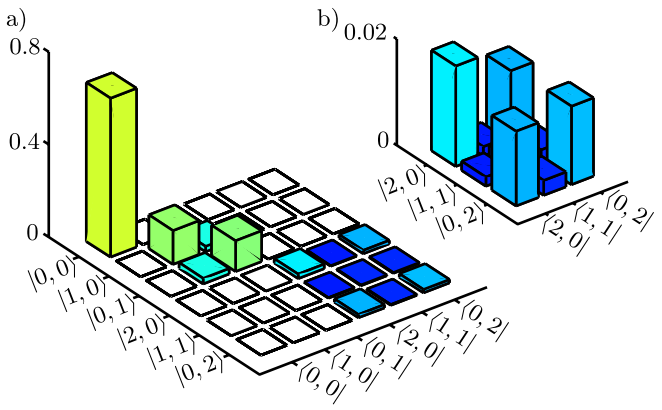

FIG. 3 (color online). Reconstructed heralded quantum state. (a) The absolute value of the density matrix including vacuum, one-, and two-photon subspaces. (b) An enlargement of the two-photon subspace. $|m, n\rangle$ denotes m diagonally (+ 45°) polarized photons and n antidiagonally (− 45°) polarized photons. Bars are colored according to their magnitude.

whole state including lower photon number subspaces is known however, the correct η_p, given by the overlap of the reconstructed state with the HB(2) state, can be calculated as $\eta_p = 0.031$. Applying the bound in [8] leads to $V_{\text{th}} = 1/\sqrt{\eta_p N_d} = 4.02$, which is unphysical. So, by this analysis, we cannot beat the SQL. The above thresholds are based on post-selection and renormalization or neglect both channel transmissivity and detector efficiencies, significantly underestimating the resources required to reach a given precision. Heralding a characterized state affords a complete reckoning of the resources used by counting all states put into the interferometer. f and η can then be estimated experimentally, allowing V_{th} to be calculated according to Eq. (1). f is determined from the ratio of fourfold coincidences to heralding events, giving $f = 0.0047 \pm 0.0001$ and $\eta\eta_d = \sqrt{f/\eta_p} = 0.39$. For our detector $\eta_d = 0.45$, $\eta = 0.87$, resulting in $V_{\text{th}} = \sqrt{\eta/Nf} = 9.57$, an even higher threshold on visibility, showing that we cannot beat the SIL. This explicitly shows that to unequivocally demonstrate performance beyond the classical limit, all system inefficiencies must be characterized.

Equation (1) and the analysis above are based on the FI and are valid only for $N00N$ states. To assess the value of a state for metrology, however, the QFI can be calculated and compared to the SIL. For our state, $F_Q = 0.079$, giving a QCRB $\Delta\phi \geq 3.56/\sqrt{\nu}$. For a classical state with the same average photon number as the reconstructed state, $\Delta\phi_{\text{SIL}} = 1.81/\sqrt{\nu}$, showing again that, despite the implications of the post-selected and renormalized analyses above, the classical limits to precision can never be surpassed with this state and arbitrary measurements.

Going beyond the classical performance limit with realistic quantum sensors requires stringent bounds on throughput, probe-state preparation and detection efficiencies. For heralded $N00N$ states, $f = \eta_p(\eta\eta_d)^N$ must satisfy $f \geq \eta/NV^2$. For the ideal two-photon situation ($V = 1$) this implies $\eta_p\eta\eta_d^2 \geq 1/2$. This benchmark for heralded two-photon states provides a challenging goal to achieve to surpass the classical limit. Even for perfect detectors ($\eta_d = 1$), this would require $\eta_p\eta \geq 1/2$. Conversely, perfect preparation and transmission ($\eta_p\eta = 1$) implies that detectors must have $\eta_d \geq 1/\sqrt{2}$. To our knowledge, the above criteria have not yet been demonstrated together in a single experiment.

Quantum photonics using feasible laboratory technology has the potential to surpass the performance of classical techniques. Nonclassical behavior may be present in an experiment, but does not necessarily imply improved performance beyond classical limits. Here we have laid out an explicit approach to compare experimental results for precision metrology, which requires complete knowledge of the input state and number of experimental trials. We have demonstrated a scalable method to generate heralded entangled states of light for precision phase estimation, a key step to demonstrating a real-world improvement over the SQL. By fully characterizing this source we have calculated the ultimate precision that can be obtained and in doing so we have put bounds on the sensor parameters required for quantum-enhanced phase estimation to be viable.

The authors thank N. Langford, R. Adamson, K. Banaszek, and J. Lundeen for discussions. This work was supported by the EC integrated project Q-ESSENCE, US European Office of Aerospace Research (FA8655-09-1-3020), EPSRC (EP/H03031X/1), and the Royal Society.

[1] V. Giovannetti and S. Lloyd, Science **306**, 1330 (2004).
[2] V. Giovannetti, S. Lloyd, and L. Maccone, Phys. Rev. Lett. **96**, 010401 (2006).
[3] S. L. Braunstein and C. M. Caves, Phys. Rev. Lett. **72**, 3439 (1994).
[4] U. Dorner *et al.*, Phys. Rev. Lett. **102**, 040403 (2009).
[5] A. Datta *et al.*, Phys. Rev. A **83**, 063836 (2011).
[6] S. F. Huelga *et al.*, Phys. Rev. Lett. **79**, 3865 (1997); A. Shaji and C. M. Caves, Phys. Rev. A **76**, 032111 (2007); A. M. Rubin and S. Kaushik, *ibid.* **75**, 053805 (2007); S. D. Huver, C. F. Wildfeuer, and J. P. Dowling, *ibid.* **78**, 063828 (2008); G. Gilbert, M. Hamrick, and Y. S. Weinstein, J. Opt. Soc. Am. B **25**, 1336 (2008).
[7] M. W. Mitchell *et al.*, Nature (London) **429**, 161 (2004); B. L. Hig-gins *et al.*, *ibid.* **450**, 393 (2007); H. S. Eisenberg *et al.*, Phys. Rev. Lett. **94**, 090502 (2005); K. J. Resch *et al.*, *ibid.* **98**, 203602 (2007); T. Nagata *et al.*, Science **316**, 726 (2007); B. J. Smith *et al.*, in *CLEO/QELS* (IEEE, New York, 2008), Vol. 1–9, p. 3044; Opt. Express **17**, 13516 (2009); J. C. F. Matthews *et al.*, Nat. Photon. **3**, 346 (2009); H. Kim, H. S. Park, and S.-K. Choi, Opt. Express **17**, 19720 (2009); J. C. F. Matthews *et al.*, arXiv:1005.5119v1.

[8] K. J. Resch *et al.*, Phys. Rev. Lett. **98**, 223601 (2007).
[9] I. Afek, O. Ambar, and Y. Silberberg, Science **328**, 879 (2010).
[10] B. C. Sanders and G. J. Milburn, Phys. Rev. Lett. **75**, 2944 (1995); A. N. Boto *et al.*, *ibid.* **85**, 2733 (2000); J. J. Bollinger *et al.*, Phys. Rev. A **54**, R4649 (1996).
[11] See Supplemental Material at http://link.aps.org/supplemental/10.1103/PhysRevLett.107.113603 for further calculations and experimental details.
[12] M. J. Holland and K. Burnett, Phys. Rev. Lett. **71**, 1355 (1993).
[13] J. A. Dunningham, K. Burnett, and S. M. Barnett, Phys. Rev. Lett. **89**, 150401 (2002).
[14] P. J. Mosley *et al.*, Phys. Rev. Lett. **100**, 133601 (2008).
[15] D. Achilles *et al.*, Opt. Lett. **28**, 2387 (2003).
[16] N. L. Thomas-Peter, B. J. Smith, and I. A. Walmsley, in *CLEO/QELS* (IEEE, New York, 2009), Vol. 1–9 p. 2430.